

Free-exciton diffusion and decay in zero-stress Ge

J. C. Culbertson

Naval Research Laboratory, Washington, D.C. 20375-5000

R. M. Westervelt

Division of Applied Sciences and Department of Physics, Harvard University, Cambridge, Massachusetts 02138

E. E. Haller

*Lawrence Berkeley Laboratory, University of California, Berkeley, California 94720**and Department of Material Science and Engineering, University of California, Berkeley, California 94720*

(Received 8 April 1986)

We report the first direct measurement of the free-exciton (FE) diffusivity D_x in germanium. The evolution in time of spatial profiles of FE luminescence were measured. From these FE density profiles we determined the diffusivity $D_x(4.2\text{ K}) \approx 300\text{ cm}^2\text{s}^{-1}$ which is limited by phonon scattering, and the surface recombination velocity $S \approx 3000\text{ cm s}^{-1}$, and an FE lifetime $\tau_x \approx 27\text{ }\mu\text{s}$ for dislocation free Ge and $\tau_x \approx 12\text{ }\mu\text{s}$ for dislocated Ge with surface recombination effects on these τ_x excluded. Evidence is presented which suggests that the FE recombination velocity S at a crystal surface is not sensitive to the detailed character of that surface. It is concluded that previous measurements could have been dramatically affected by the surface recombination of FE, especially those measurements made on crystals whose dimensions are on the order of the FE diffusion length. An FE-phonon scattering time $\tau_p(4.2\text{ K}) \approx 2 \times 10^{-10}\text{ s}$ is deduced from the measured diffusion constant.

I. INTRODUCTION

The quantities determined from experimental studies of free-exciton (FE) diffusion depend on the dominant scattering mechanism. If the dominant scattering mechanism for FE diffusion is FE-FE collisions, then the FE-FE collision cross section can be determined. If the dominant FE scattering mechanism involves collisions with phonons, then an FE-phonon scattering time τ_p can be determined. If the former case (self-diffusion) is physically realizable, then the potential exists to study both types of diffusion; by reducing the FE density, FE-FE collisions become less probable and other FE scattering mechanisms will become dominant. If self-diffusion is not observed, then one can use the maximum attainable FE density to set limits on the FE-FE scattering cross section.

There are good reasons to be suspicious of the experiments claiming to measure D_x that have been published prior to this¹ work. The basic problem is that people have not been measuring what they have intended to measure: Diffusion has been measured with electron-hole liquid droplets (EHD's) present; the EHD's act as an FE source which seriously perturbs the FE spatial distribution. Or, the FE diffusion length L_x [$L_x = (D_x \tau_x)^{1/2}$] is measured and D_x is calculated using a separate measurement of the FE lifetime τ_x . The FE lifetimes used for such calculations have been suspect, as will be explained later. Finally, care must be taken that the transport studied is diffusive transport and not forced transport. As an illustration, consider the related problem of EHD diffusion. The early experiments² purporting to measure the EHD diffusivity D_d yielded a spread of values from 0.1 to 500

cm^2s^{-1} . Westervelt *et al.*,³ by cleverly making use of the optical hysteresis in the formation of EHD's, were able to monitor an essentially fixed set of EHD's for periods of hours using low-intensity photoexcitation. They found an upper limit $D_d \leq 10^{-9}\text{ cm}^2\text{s}^{-1}$. The reason for the discrepancy between this result and earlier measurements lies in the use of intense photoexcitation sources in the earlier work. The transport observed was forced transport, not diffusive transport. Drops were propelled from the photoexcited region by forces, notably the phonon wind, due to the high excitation levels used.

The main portion of this experiment involves measuring spatial profiles of Ge luminescence intensity I_x at various times after a GaAs laser photoexcites a Ge crystal. The FE will diffuse into the crystal away from the excitation surface. If the surface does not act as a recombination site for FE, the FE distribution will peak at the excitation surface where it has zero slope. If there is surface recombination then the FE distribution will peak inside the crystal. From these FE density profiles an FE diffusivity is deduced, surface recombination is characterized, and an exciton lifetime, with surface effects excluded, is found. The determination of the diffusivity from the data does not depend on the FE lifetime.

The FE radiative lifetime in Ge is expected to be $\tau_{rx} \sim 500 \pm 200\text{ }\mu\text{s}$. This is based on the observation that the EHD lifetimes measured for a variety of Ge crystals is $\tau_L = 40 \pm 5\text{ }\mu\text{s}$. This lifetime is taken to be an intrinsic property of the electron-hole liquid (EHL) in zero-stress Ge. A further measurement⁴ has deduced the radiative efficiency of the EHL to be $e_{rL} = \tau_L / \tau_{rL} = 0.33$. Finally, Westervelt⁵ and Westervelt *et al.*⁶ have measured

$\tau_{rx}/\tau_{rL}=4.1\pm 1.8$. The above τ_{rL} then follows straightforwardly. Actually measurements of FE lifetimes have varied from 1 to 20 μs . The large nonradiative recombination rate is not yet completely understood. Impurities, dislocations, and surfaces may act as recombination sites. To study FE decay in bulk Ge, one needs to be aware of the relative importance of surface recombination. In this paper we will evaluate the importance of surface recombination.

II. EXPERIMENTAL DETAILS

The measurements in this chapter were made at 4.2 K unless it is stated otherwise. The experimental geometry is illustrated in Fig. 1. A single-junction GaAs laser diode is pulsed (pulse width $\leq 2 \mu\text{s}$, pulse rate $\sim 4 \text{ kHz}$). The light (wavelength $\approx 0.865 \mu\text{m}$) escaping from the length of the diode junction is focused as a stripe on the face of a Ge crystal. Luminescence leaving the crystal through a surface at right angles to the excitation surface is routed to a spectrometer. The spectrally resolved luminescence is then detected by a cooled Ge photodiode. For time-resolved measurements a boxcar integrator was used. The response time of the Ge photodiode detector with its preamp was 2 μs .

Because accurate imaging was a high priority, special care was taken to prepare flat highly polished crystal surfaces. The dimensions of the crystals used were $\sim 4 \times 8 \times 8 \text{ mm}^3$. A square face was photoexcited and luminescence leaving a rectangular face was collected. In cutting the samples out of larger pieces of Ge crystal, this rectangular face was optically polished before a cut was made for the excitation surface. This avoided the rounding of the viewing surface near the corner with the excita-

tion surface that otherwise would have occurred during polishing.

Another concern was internally reflected luminescence escaping out the edges of the crystal. On crystals with etched surfaces there are large "edge effects" on spatial scans of luminescence. To minimize these edge effects none of the crystal surfaces were etched. Later in the experiment the excitation surface alone was etched (with a 3:1 mixture of HNO_3 and HF) in order to see the effect on the surface recombination of FE's.

The spatial resolution for the optics used was 0.2 mm for luminescence coming from the middle of the crystal where the laser stripe illuminated the crystal. The depth of field was 3 mm. Thus, the luminescence that passes through the spectrometer slit and is detected came from a $\sim 0.2\text{-mm}$ -thick slice of the crystal. Stripe excitation was chosen because it minimizes the spreading of the measured FE spatial distribution due to the finite depth of field.

III. FREE-EXCITON DIFFUSION MECHANISM

To determine whether the self-diffusion of FE at 4.2 K is important for the FE densities n_x of this experiment, FE diffusion profiles were compared for a number of laser-pulse energies. The diffusion profiles should depend on the laser-pulse energy for self-diffusion ($D_x \propto n_x^{-1}$). Profiles corresponding to a fixed time delay from the laser pulse were observed to have the same shape and width for over a factor of ten variation in pulse energy. For the highest pulse energy used the maximum n_x was just below the n_x where EHD's would still be present ($n_x \sim 10^{14} \text{ cm}^{-3}$). This indicates that the self-diffusion of FE's is not the dominant diffusion mechanism. Further evidence supporting this finding will be discussed in Sec. VI (Results and Conclusions). This finding greatly simplifies the treatment of experimental FE diffusion profiles.

IV. A SIMPLE INTERPRETATION OF FE DIFFUSION PROFILES

The scattering mechanism responsible for the diffusion occurring in this experiment does not depend on the FE density n_x . This means that the diffusion of two FE distributions superimposed on one another proceeds identically to the sum of the ways each separate distribution would diffuse. Thus the diffusion profiles corresponding to one laser stripe should be identical to the diffusion profiles corresponding to a continuous distribution of laser stripes across the excitation surface. The solution to a one-dimensional diffusion equation should describe the diffusion profiles measured in this work.

The one-dimensional diffusion equation is

$$D_x \frac{d^2 n_x}{dy^2} - \frac{dn_x}{dt} = \frac{n_x}{\tau_x} . \quad (1)$$

It will be assumed that τ_x is independent of n_x . A semi-infinite medium will be assumed. As a boundary condition for the excitation surface it will be assumed that the flux of FE into the surface is proportional to the FE concentration $n_x(0)$ at the surface,

EXPERIMENTAL GEOMETRY

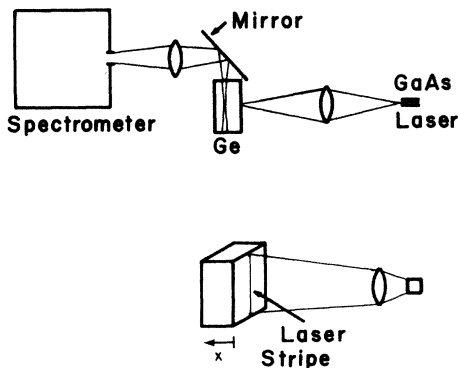


FIG. 1. Experimental Geometry. A stripe of radiation from a GaAs laser diode's junction is pulsed onto an ultrapure $8 \times 8 \times 4 \text{ mm}^3$ Ge crystal at $T=4 \text{ K}$. Luminescence leaving the side of the crystal is routed to the detection apparatus. Spatial scans are made by translating the output lens.

$$J_{\text{into surface}} = D_x \left. \frac{dn_x}{dy} \right|_{y=0} = S n_x \Big|_{y=0}. \quad (2)$$

Here, y increases going into the crystal, and S is called the surface recombination velocity. For an isotropic velocity distribution, simple kinetic and geometric arguments predict that S can be no larger than one-fourth the aver-

age thermal velocity.

Making the substitution,

$$n_x(y,t) = n(y,t)e^{-t/\tau_x}$$

into Eq. (1) and using a Laplace transform to solve the resulting equation we obtain,

$$n_x(y,t) = n(y,t)e^{-t/\tau_x} = P \left[\frac{\exp(-y^2/4D_x t)}{(\pi D_x t)^{1/2}} - \frac{S}{D_x} \exp\left(\frac{yS}{D_x} + \frac{S^2 t}{D_x}\right) \operatorname{erfc}\left(\frac{S\sqrt{t}}{(D_x)^{1/2}} + \frac{y}{(4D_x t)^{1/2}}\right) \right] e^{-t/\tau_x}. \quad (3)$$

To assess the importance of surface recombination we integrate over the volume of the semi-infinite medium. Defining

$$N_x = \int_0^\infty n_x(y,t) dy \quad \text{and} \quad N = \int_0^\infty n(y,t) dy,$$

the result is

$$N_x = N e^{-t/\tau_x} = P \left\{ e^{S^2 t/D_x} \operatorname{erfc}[(S^2 t/D_x)^{1/2}] \right\} e^{-t/\tau_x}. \quad (4)$$

The measured decay rate is given by

$$\frac{1}{\tau_{\text{apparent}}} = -\frac{dN_x}{dt} / N_x = \frac{1}{\tau_x} + \left[-\frac{dN}{dt} / N \right] \equiv \left[\frac{1}{\tau_x} \right]_{\text{bulk}} + \left[\frac{1}{\tau_x} \right]_{\text{surface}}.$$

Evaluating $(\tau_x)_{\text{surface}}$ using Eq. (4) yields

$$(\tau_x)_{\text{surface}} = D_x / S^2 / \left[\frac{e^{-S^2 t/D_x}}{(S^2 t \pi / D_x)^{1/2} \operatorname{erfc}[(S^2 t/D_x)^{1/2}]} - 1 \right]. \quad (5)$$

The manner in which $(\tau_x)_{\text{surface}}$ varies in time is determined entirely by the ratio D_x/S^2 .

V. DATA AND DISCUSSION

This experiment was performed on two crystals: Crystal 1 (dislocation-free p type), and Crystal 2 (dislocated n type). The data obtained using Crystal 1 will be discussed first.

First, the laser-pulse energy was increased to just above the threshold for electron-hole droplets (EHD's) creation. Figure 2 shows three spatial profiles of EHL luminescence for various times after the laser pulse. The EHL luminescence is seen to decay in place much faster than the 40- μ s lifetime of bulk EHL. This is due to the creation of small EHD's. Because of large surface-to-

volume ratios, their decay is dominated by the surface evaporation of e - h pairs. The FE and EHD spatial profiles (d) and (c) indicate that FE's dominate the behavior of the system after a 12.5- μ s delay. This is especially clear when one recalls from the introduction above that the EHL radiative decay rate is four times larger than the FE radiative decay rate. To plot the curves (a)–(d) such that a given amplitude corresponds to the same number of electron-hole pairs, curve (d) would have to be multiplied by four. Also, the rate at which the decaying EHD's give off e - h pairs is not sufficient to have prevented the peak

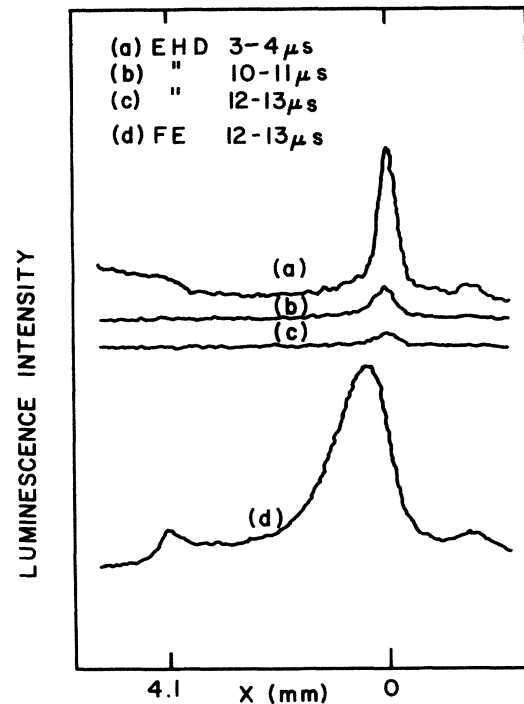


FIG. 2. Spatial scans of electron-hole droplet (EHD) luminescence intensity (a)–(c) at times up to 12 μ s after the laser pulse, when the first free-exciton (FE) profile (d) is recorded. All profiles are drawn to the same scale.

of the FE distribution from moving inside the crystal. Finally, we emphasize that the EHD's are all decaying in place very close to the crystal surface. This is an indication of the low-excitation powers used. The powers are low enough that the phonon wind is not strong enough to propel EHD's. Arguments concerning whether the phonon wind need be considered for FE in this experiment are given in the Sec. VI.

Figure 3 shows the spatially integrated FE and EHL luminescence decay curves corresponding to the same laser-pulse energy as Fig. 2. The EHL luminescence decays much faster than the 40- μ s lifetime of bulk EHL. The EHL luminescence disappears into the noise 15 μ s after the laser pulse. The FE decay rate slows continuously until about 30 μ s after the laser pulse. After 30 μ s the FE decay appears to be exponential with an apparent lifetime $(\tau_x)_{\text{apparent}} = 27 \mu$ s. Within the 15- μ s span of time (starting after the EHD's are gone) in which the FE decay rate changes, the spatially integrated FE luminescence intensity has dropped by almost half a decade. A larger initial FE decay rate is consistent with an initially larger FE decay at the crystal surface. As time progresses, the FE distribution moves into the crystal (see Fig. 4) and surface decay becomes less dominant. We believe that the FE decay is starting to become faster than exponential toward the end of the observable decay due to the shifting of the free carrier (FC)-FE equilibrium toward FC as the concentrations of FC and FE decrease.

Free-exciton spatial profiles, for times ranging from 13 to 80 μ s after the laser pulse, are plotted in Fig. 4. The FE's are seen to move into the crystal away from the excitation surface on the right (indicated by arrows). The back face of the crystal is clearly indicated by the small

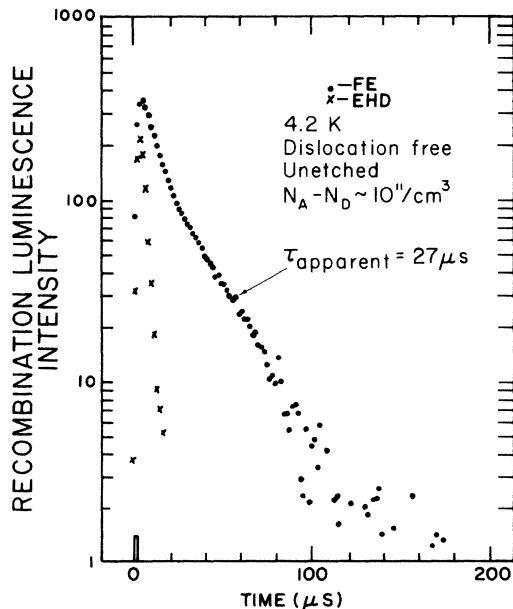


FIG. 3. Free-exciton (FE) and electron-hole droplet (EHD) luminescence decay. The width of the tickmark at $t = 0$ is the 2 μ s pulse width of the exciting laser. Crystal 1.

peak. This peak is due to internally reflected light escaping through the corner of the crystal (edge effect). As was expected, the FE distribution is pulled down near the excitation surface. By 25 μ s after the laser pulse, the peak of the FE distribution has moved $\frac{3}{4}$ mm into the crystal and FE's are starting to reach the back surface of the crystal (which was not taken into account in the preceding section). By 40 μ s, the back surface is starting to significantly effect the time evolution of the diffusion profiles and perhaps the FE decay. By 80 μ s, the distribution of FE's between the crystal surfaces is becoming fairly symmetric. When the rates of FE decay at the crystal's front and back surfaces become comparable (an asymptotic diffusion profile has been reached), then the increasing of the apparent FE lifetime $(\tau_x)_{\text{apparent}}$ with time will stop. A mechanism such as this quite conceivably could have affected FE lifetime measurements made using small Ge crystals.

Analogous decay curves and diffusion profiles, measured using Crystal 2 (~ 350 dislocations cm^{-2}), are plotted respectively in Figs. 5 and 6. The apparent FE life-

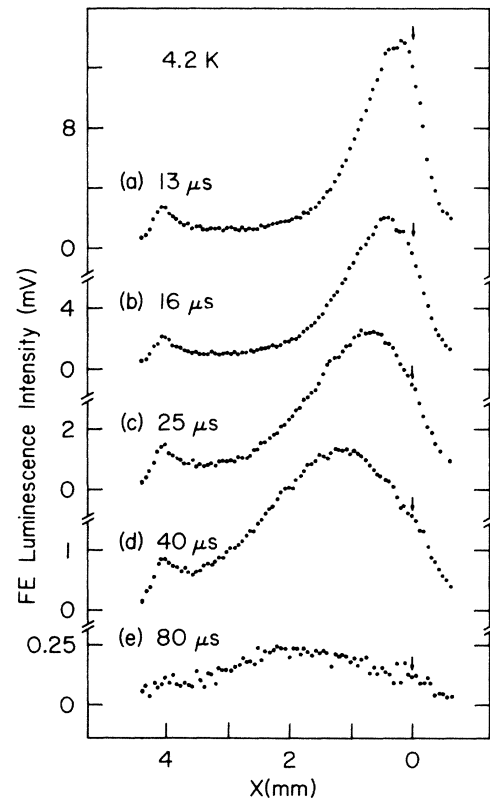


FIG. 4. Free-exciton (FE) luminescence is viewed through a surface at right angles to the photoexcited surface at various times after the laser pulse. These data show the FE diffuse into the crystal from the excitation surface (indicated by the arrows on the right) toward the rear surface (indicated by the peak due to escaping internally reflected luminescence). The FE density near the surface is pulled down by surface recombination. Crystal 1.

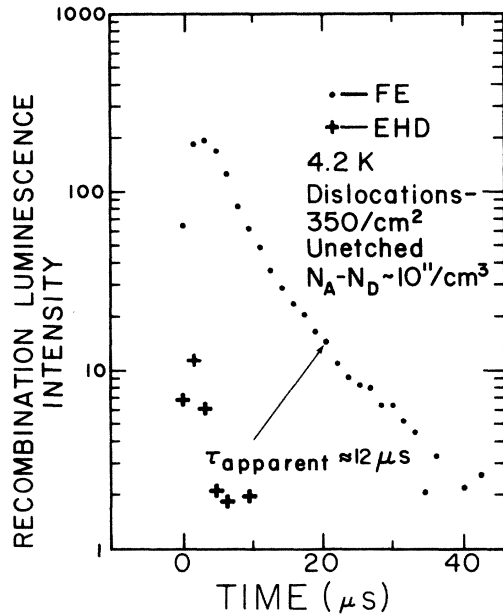


FIG. 5. Free-exciton (FE) and electron-hole droplet (EHD) luminescence decay. Crystal 2.

time of $12 \mu\text{s}$ suggests that dislocations are active as recombination centers. This correlation has been independently verified by a group of Soviet scientists.^{7,8} The diffusion profiles exhibit the same features as those for Crystal 1.

VI. RESULTS AND CONCLUSIONS

The data were fitted to Eq. (5), the solution for a δ -function excitation just inside the crystal surface. The fit-

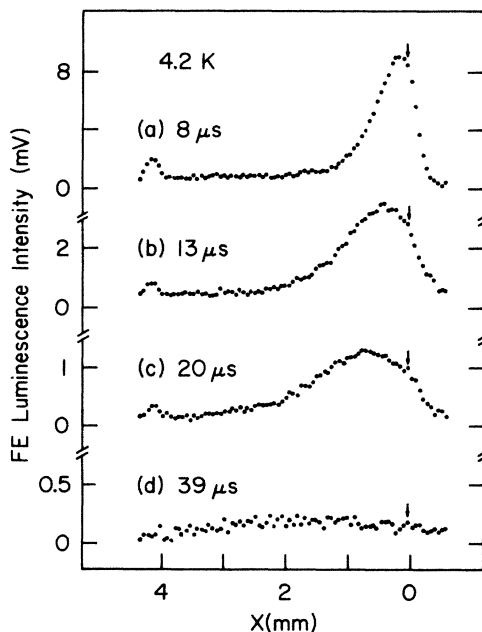


FIG. 6. Time-resolved free-exciton (FE) spatial profiles in response to pulsed photoexcitation. Crystal 2.

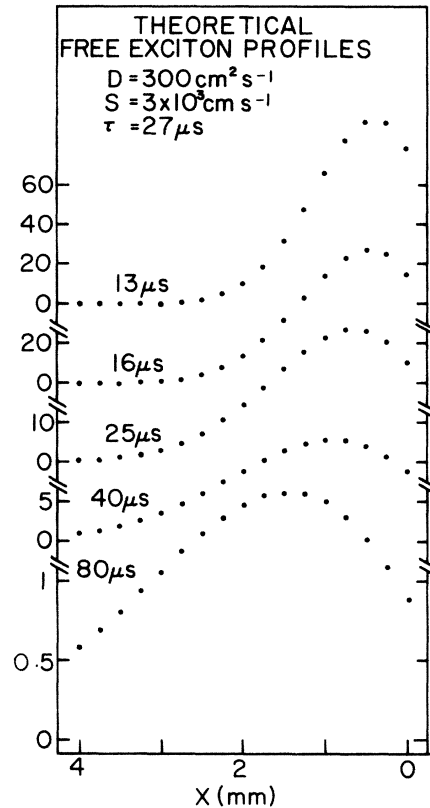


FIG. 7. Theoretically generated free-exciton spatial profiles using the best fit parameters for the data of Fig. 4.

ting parameters were D_x , S , and the time in Eq. (3) corresponding to the first measured diffusion profile. These parameters were chosen to optimize the agreement between the position and width of the FE diffusion profiles as well as the slope at the excitation surface. The theoretical [Eq. (3)] diffusion profiles that result from fitting the diffusion profiles of Fig. 4 are plotted in Fig. 7.

It should be noted at this point that the above experiments were repeated on the same two crystals, but with the excitation surfaces etched. The resulting decay curves and diffusion profiles were identical to those measured using unetched surfaces. However, it took one-seventh as much laser-pulse energy to reach the EHL threshold. This observation would seem to support an argument that the surface recombination velocity S is determined by the fact that there is a surface and not so much the detailed character of that surface (at least for the surface preparations used here). Furthermore, the effect that crystal damage at the surface has on the laser-pulse energy necessary to create a given number of e - h pairs can be understood through absorption length effects: The excitation light incident on a polished surface that actually makes it through the damaged layer is attenuated by an amount determined by the absorption length of the radiation and the thickness of the layer. For the GaAs laser used here this corresponds to a $1\text{-}\mu\text{m}$ -thick layer of damaged crystal (consistent with the grit sizes used for polishing).

The fit corresponding to Fig. 7 used

$$D_x = 300 \text{ cm}^2 \text{ s}^{-1}$$

and

$$S = 3000 \text{ cm s}^{-1}.$$

These results will be discussed below after a simple theoretical discussion of FE diffusion mechanisms and a discussion of other measurements.

The two most important scattering mechanisms that limit the diffusion of FE in ultrapure Ge at liquid helium temperatures are FE-FE scattering (self-diffusion) and scattering with thermal LA phonons.

The FE diffusivity D_x is given in terms of an FE scattering time τ by

$$D_x = \frac{k_B T}{m_x} \tau. \quad (6)$$

In the case of *self-diffusion*, the mean time between FE scattering is given by $\tau = L / \langle v \rangle$, where $L = 1 / (2^{1/3} n_x \sigma)$ is the mean free path between FE collisions and $\langle v \rangle = [8k_B T / (\pi m_x)]^{1/2}$ is the average speed of an FE. Here, σ is the total cross section for FE-FE scattering, n_x is the FE density, and $m_x = 0.436 m_0$ is the FE translational mass.^{9,10} Thomas *et al.*¹¹ have determined an effective FE-FE collision radius of 220 ± 80 Å from the collision broadening of the FE spectra lineshape. A radius of 220 Å implies that the self-diffusion of FE is substantial for the conditions of our diffusion experiments. Because the diffusion profiles we measure are independent of excitation power (i.e., of FE density) we believe that the correct collision radius is at least on the low end of their error limits. This is close to the FE Bohr radius a_x which we will use as the collision radius in the discussion below.

Assuming $\sigma = \pi a_x^2$, the diffusivity for the self-scattering of FE at zero stress is

$$D_{xs} = (3 \times 10^{16} \text{ cm}^{-1} \text{ s}^{-1} \text{ K}^{-1/2}) \frac{T^{1/2}}{n_x}. \quad (7)$$

Consider the case where the mechanism for FE diffusion is scattering by LA phonons. The mean scattering time for FE's with LA phonons is¹²

$$\tau_p = \frac{2\sqrt{2}}{3} \pi \frac{\rho s^2 \hbar^4}{m_x^{3/2} E^2 (k_B T)^{3/2}}. \quad (8)$$

For Ge, with $m_x = 0.436 m_0$, density $\rho = 5.32 \text{ g cm}^{-3}$, sound velocity $s = 1.6 \times 10^5 \text{ cm s}^{-1}$, and deformation potential $E = 2 \text{ eV}$,¹³ this yields

$$\tau_p \approx (3.8 \times 10^{-9} \text{ K}^{3/2} \text{ s}) T^{-3/2}.$$

Measurements by Tamor and Wolfe¹⁴ for τ_p in Si were found to be in good agreement with Eq. (8). Tamor and Wolfe¹⁵ have measured $\tau_p(2\text{K}) \approx 0.53 \pm 0.07 \text{ ns}$ for the EHL in Ge. The equivalence of τ_p for the EHL and τ_p for the FE has been demonstrated convincingly [Ref. 2, p. 143]. This implies that the above equation for τ_p is a factor of 2.5 high. Measurements of τ_p for electrons and holes separately have also been made. Hensel and Suzuki¹⁶ have measured $\tau_p(1.8 \text{ K}) \sim 5 \times 10^{-10} \text{ s}$ for holes, while Ito *et al.*¹⁶ have measured $\tau_p(1.8 \text{ K}) \sim 10^{-9} \text{ s}$ for electrons. These measurements are in the same ratio as

their density of states masses^{1,17} to the $\frac{3}{2}$ power. This is expected from Eq. (8). However, the magnitudes predicted by Eq. (8) are a factor of 4.4 high. We take the measurement of τ_p by Tamor and Wolfe¹⁵ as the most accurate value, so we will use the τ_p of the above equation scaled down by 2.5,

$$\tau_p \approx [(1.5 \pm 0.2) \times 10^{-9} \text{ K}^{3/2} \text{ s}] T^{-3/2}. \quad (9)$$

With this scaled-down τ_p the predicted FE diffusivity due to scattering with LA phonons is

$$D_{xp} = [(530 \pm 70) \text{ cm}^2 \text{ s}^{-1} \text{ K}^{1/2}] T^{-1/2}. \quad (10)$$

To combine diffusivities due to different scattering mechanisms, the scattering rates (τ^{-1}) are added. Thus diffusivities [see Eq. (6)] are added reciprocally. So $1/D_x = 1/D_{xs} + 1/D_{xp}$ which yields

$$D_x = \{ [(1.9 \pm 0.25) \times 10^{-3} \text{ cm}^{-2} \text{ s K}^{-1/2}] T^{1/2} + (3.3 \times 10^{-17} \text{ cm s K}^{1/2}) n_x T^{-1/2} \}^{-1}. \quad (11)$$

Pokrovskii and Svistunova¹⁸ claim to have measured $D_x = 1500 \text{ cm}^2 \text{ s}^{-1}$ at 3 K. The largest possible value for D_x from Eq. (11) is $D_x = D_{xp} = 306 \text{ cm}^2 \text{ s}^{-1}$, a factor of 5 smaller than their result. In their experiment they measured the diffusion length L_x and the FE lifetime τ_x . They inferred $D_x = L_x^2 / \tau_x$. The EHL lifetime reported was low by a factor of 2. They used the same measurement technique to measure the EHL and FE lifetimes. Furthermore, we are not convinced that the ionizing electric fields they used to make their measurements did not interfere with the processes they were trying to measure.

The D_x we have determined from our measured FE diffusion profiles are consistent with the phonon scattering diffusivity $D_{xp} = (260 \pm 35) \text{ cm}^2 \text{ s}^{-1}$ predicted from Eq. (10). The diffusion profiles were consistent with those expected for diffusion mediated by LA phonons, but it is difficult to rule out the existence of a small component of D_{xs} . The maximum D_{xs} that Eq. (7) predicts for this experiment is given by the following considerations: The FE density is determined from a calorimetry measurement of the laser-pulse energy, and an effective volume occupied by the FE. An effective volume can be determined by examining the spatial extent of the first diffusion profile. This yields a rough estimate for the peak FE concentration of $n_x \sim 10^{14} \text{ cm}^{-3}$. The value of D_{xs} predicted by Eq. (7) is $D_{xs}(4.2 \text{ K}) = 615 \text{ cm}^2 \text{ s}^{-1}$. Combined with $D_{xp}(4.2 \text{ K}) = 260 \text{ cm}^2 \text{ s}^{-1}$ from Eq. (10), the total diffusivity is predicted to be $D_x = 183 \text{ cm}^2 \text{ s}^{-1}$. This is somewhat low compared to the value determined in this work. This indicates that there is room for improvement in the FE-FE scattering cross section appropriate for the self-diffusion of FE's.

For the crystals studied here D_x is not dependent on impurity type or concentration, or on dislocation density. This behavior is consistent with diffusion mediated by LA phonons as given by Eq. (10) which predicts $D_x \propto T^{-1/2}$. This trend with temperature is qualitatively supported by separate measurements we made of the diffusion length L_x from spatial profiles produced by steady state surface excitation (small absorption length). The diffusion lengths measured increased with decreasing temperature.

The FE lifetimes were not measured for lower temperatures, but the trend holds as long as the FE lifetime does not increase with temperature. At 3 K, assuming τ_x is the same as at 4.2 K, the D_x that we determine from these measurements is about one-fourth of the value $D_x = 1500 \text{ cm}^2 \text{ s}^{-1}$ discussed above.¹⁸ The L_x resulting from our steady state measurement at 4.2 K when combined with our measured FE lifetime $\tau_x = 27 \mu\text{s}$ is consistent with the value $D_x = 300 \text{ cm}^2 \text{ s}^{-1}$ reported here. The steady state L_x was measured for FE densities an order of magnitude lower than were used in the pulsed experiment. This is further support for the contention that self-diffusion is negligible. This would also seem to indicate that forced transport (e.g., phonon wind) is not involved. That is, of course, barring the unlikely situation in which the opposing effects of phonon wind and self-diffusion cancel or mask the effect of each other. These observations support the hypothesis that FE diffusion, for the conditions specified in this work, is mediated by LA phonons and furthermore that the $(\tau_x)_{\text{apparent}}$ measured in the exponential decay region is indeed the bulk Ge FE lifetime τ_x . The value of the FE-phonon scattering time implied by $D_x = 300 \text{ cm}^2 \text{ s}^{-1}$ is determined from Eq. (6) using the most recent spherical average FE translational mass^{9,10} ($m_x = 0.436 m_0$) to be $\tau_p = 2 \times 10^{-10} \text{ s}$ at 4.2 K. When scaled for temperature using Eq. (9), this value is in agreement with the τ_p of Tamor and Wolfe¹⁵ which was measured at 2 K.

The value of $S = 3000 \text{ cm s}^{-1}$ for FE at a crystal surface should be compared with $S \sim 10^2 \text{ cm s}^{-1}$ for free carriers (attributed to Hensel). The FE surface recombination velocity should be larger than that for free carriers, because carriers bound in FE's bring their recombination partners with them to the surface. Furthermore, S should be less than one-fourth the average FE velocity as required by simple kinetic and geometric arguments. This provides the upper bound $S \leq 5 \times 10^5 \text{ cm s}^{-1}$. The value of S reported here is consistent with the expected limit on its value.

Finally, within the accuracy of the D_x and S and the

accuracy of the FE decay data (Fig. 3), there is agreement between the predicted $(\tau_x)_{\text{apparent}}$ from Eq. (5) and those measured from Fig. 3.

In concluding, we note that the effects of surface recombination should be carefully considered when measuring FE decay rates. If the FE decay rate τ_x^{-1} in the bulk material is smaller than or comparable to the surface decay rate, then lifetimes significantly shorter than τ_x will be measured. Lifetime measurements made using samples whose dimensions are comparable to the diffusion length or smaller can be dramatically effected. Lifetime measurements can also give erroneous results if not enough time has elapsed to allow the FE distribution to move away from the crystal surface. Consider, for example, a lifetime measurement⁵ made using a thinner ($2 \times 8.5 \times 8.5 \text{ mm}^3$) piece of Ge (cut from the same stock as Crystal 1) which yielded a value $\tau_x = 7.7 \mu\text{s}$. For Crystal 1 we have measured the FE decay out to longer times and find $\tau_x = 27 \mu\text{s}$. The decay of FE in a small sample can even look exponential and still be dramatically effected by surface recombination. All that is required for exponential FE decay is that the rate at which FE's decay be proportional to the number of FE's. If a spatially symmetric diffusion profile is reached, it will decay maintaining its shape. Thus the concentration of FE's at a surface becomes proportional to the total number of FE's. Thus the rate of surface decay is proportional to the total number of FE's and the measured exponential decay rate is given by the sum of the bulk and surface decay rates—both of which are constant.

ACKNOWLEDGMENTS

The experimental part of this paper was performed at the University of California at Berkeley where it was supported by the Director, Office of Energy Research, Office of Basic Energy Science, Material Sciences Division of the U.S. Department of Energy under Contract No. DE-AC03-76SF00098.

¹J. C. Culbertson and R. M. Westervelt, *Bull. Am. Phys. Soc.* **24**, 342 (1979); The value $D_x = 300 \text{ cm}^2 \text{ s}^{-1}$ at 4.2 K was reported at the conference.

²See reviews by T. M. Rice and by J. C. Hensel, T. G. Phillips, and G. A. Thomas, in *Solid State Physics*, edited by H. Ehrenreich, F. Seitz, and D. Turnbull, (Academic, New York, 1977), Vol. 32, and references within.

³R. M. Westervelt, J. C. Culbertson, and B. S. Black, *Phys. Rev. Lett.* **42**, 267 (1979).

⁴M. S. Skolnick and D. Bimberg, *Phys. Rev. B* **21**, 4624 (1980).

⁵R. M. Westervelt, T. K. Lo, J. L. Staehli, and C. D. Jeffries, *Phys. Rev. Lett.* **32**, 1051 (1974); **32**, 1331E (1974).

⁶R. M. Westervelt, *Proceedings of the Thirteenth International Conference on Physics of Semiconductors*, edited by F. G. Fumi (Tipographia Marves, Rome, 1976), p. 916.

⁷L. G. Goncharov, L. V. Ryabykina, and K. I. Svistunova, *Fiz. Tverd. Tela.* **19**, 2831 (1977) [*Sov. Phys.—Solid State* **19**, 1659 (1977)].

⁸Ya. A. Pokrovskii, G. M. Gavrilov, L. A. Goncharov, P. D.

Kervalishvii, and P. G. Litovchenko, *Fiz. Tekh. Poluprovodn.* **12**, 1833 (1978) [*Sov. Phys. Semicond.* **12**, 1087 (1978)].

⁹R. M. Westervelt, Ph.D. thesis, University of California, 1977.

¹⁰R. M. Westervelt, J. L. Staehli, and E. E. Haller, *Phys. Status Solidi B* **90**, 557 (1978).

¹¹G. A. Thomas, A. Frova, J. C. Hensel, R. E. Miller, and P. A. Lee, *Phys. Rev.* **13**, 1692 (1976).

¹²J. M. Ziman, *Electrons and Phonons*, (Oxford University Press, Oxford, 1960), p. 433.

¹³I. Balslev, *Phys. Rev.* **143**, 636 (1966).

¹⁴M. A. Tamor and J. P. Wolfe, *Phys. Rev. Lett.* **44**, 1703 (1980).

¹⁵M. A. Tamor and J. P. Wolfe, *Phys. Rev. B* **24**, 3596 (1981).

¹⁶R. Ito, H. Kawamura, and M. Fukai, *Phys. Rev. Lett.* **13**, 26 (1964).

¹⁷S. M. Kelso, *Phys. Rev. B* **25**, 1116 (1982).

¹⁸Ya. E. Pokrovskii and K. I. Svistunova, *Fiz. Tverd. Tela.* **13**, 1485 (1971) [*Sov. Phys.—Solid State* **13**, 1241 (1971)].